Voltage Stability Assessment of 330KV Nigeria Power System Using Continuation Power Flow Technique

I. O. Akwukwaegbu, E.N.C. Okafor, F. I Izuegbunam, M. C Ndinechi

***Abstract*— Voltage stability challenges of the Nigeria power system which stem from inadequate generation and poor power evacuation capability of the transmission facilities need not be over emphasized. The major problems confronting Nigeria power network are low voltage violations, high voltage violations and line MVA limits violations. Voltage violations occur at the buses, which suggest that voltage at the bus is less than or greater than the specified value, which may lead to voltage stability problems. This paper therefore evaluated the voltage profiles of the present 28-bus Nigeria power network via continuation power flow techniques. The results show that under normal operating conditions, all the 28-bus voltage profiles were violated as ±5% tolerance of the rated value were exceeded. It also exposed the network's poor loadability limits as well as low voltage stability indices problem.**

***Index Terms*— Low voltage violations, high voltage violations, line loadability, continuation power flow, voltage stability, p-v curve**

I. INTRODUCTION

As new sources of power are added to the Nigeria power system, an over-riding factor in the operation of the electrical network is the desire to maintain acceptable voltage level in every segment: generation, transmission, and distribution within ±5% of the rated voltage. The existing Nigeria power network comprising 5,988Km of 330KV grid transmission lines is facing the following challenges: inability to effectively dispatch generated energy to meet the load demand; large number of uncompleted transmission line projects, reinforcement/expansion projects in the power industry; poor voltage profile at the buses; inability of the existing transmission lines to wheel more than 4000MW of power at present operational conditions, in addition to voltage and frequency control problems [1,2,3,4]. The grid system in Nigeria is almost radial single circuit lines, fragile and very long transmission lines. Many of these lines experience total or partial system collapse when subjected to major disturbances and this makes voltage control difficult. Other problems include: poor network configuration in some regional work centres; ineffective control of the transmission line parameters; large numbers of overloaded transformers in the grid systems; the use of transmission lines beyond their thermal limits and activities of vandals on the 330KV transmission lines in various parts of the country. Transmission-line voltage decreases when heavily loaded and increases when lightly loaded, the phenomenon is known as line loadability. The line-loading limits are the thermal limits, the voltage-drop limit, and the steady-state stability limit. The existing power network must be transformed and expanded from radial to ring because of the high power losses associated with it and this will help to maintain the voltage profile within the acceptable range of +5% or – 5% of nominal value in the system.

Voltage stability being the ability of a power system to maintain steady voltage at all the buses in the system after being subjected to a disturbance from a giving initial operating condition; and it is dependent on the ability to maintain/restore equilibrium between load demand and load supply from the power system [5, 6].

The conventional power flow model and the continuation power flow (CPF) method are used to investigate voltage stability. The purpose of the continuation power flow is to find a continuum of power flow solution for any change in load. The general principle behind the continuation power flow is simple. It employs a predictor – corrector scheme to find a solution path of a set of power flow equations that have been reformulated to include a load parameter [7, 8, 9]. It starts from a known solution corresponding to a different value of the load parameter. This estimate is then corrected using the same Newton-Raphson technique employed by a conventional power flow. The local parameterization provides a means of identifying each point along the solution path and plays an integral path in avoiding singularity in the Jacobian.

Voltage stability is determined by computing power - voltage (P-V) curves at all the buses of the network. P-V curves are generated by executing a large number of the MATLAB/SIMULINK Power System Analysis Toolbox (PSAT) programmes that use continuation power flow (CPF) techniques for the voltage stability analysis. The P-V curves estimate the maximum loadability limits that quantify the voltage stability indices and also, determine the weak bus in the system.

The conventional power flow method failed to solve the problem of the singularity of Jacobian of a Newton-Raphson power flow at the steady state voltage stability limit. As a consequence, attempts at power flow solution or Newton-Raphson programmes near the critical point are prone to divergence and error. It is also clear that any P-V graph obtained here oscillates as it reaches the knee/critical point due to the singularity of the Jacobian. To avoid this, the continual power flow method or continuation method is used to solve this problem, which is implemented in this paper. This continuation method solved the insolvability in the conventional power flow technique.

Manuscript received June 20, 2016

I. O. Akwukwaegbu, Department of Electrical and Electronic Engineering, Federal University of Technology, Owerri, Nigeria

E.N.C. Okafor, Department of Electrical and Electronic Engineering, Federal University of Technology, Owerri, Nigeria

F. I Izuegbunam, Department of Electrical and Electronic Engineering, Federal University of Technology, Owerri, Nigeria

M. C Ndinechi, Department of Electrical and Electronic Engineering, Federal University of Technology, Owerri, Nigeria

Static voltage instability is mainly associated with reactive power imbalance. Reactive power support that the bus receives from the systems can limit loadability of that bus. If the reactive power support reaches the limit, the system will approach the maximum loading point or voltage collapse point [10].

The singularity in the Jacobian can be avoided by slightly reformulating the power flow equations and applying a locally parameterized continuation technique [7].

II. PRESENT GENERATION CAPACITY

Power supply is either a source of generation or transformation from which the power is available to meet the load demand in MW. Presently, the total installed Nigeria power generating capacity including new power plants under construction is 12,426MW, whilst the available capacity is 3,863.5MW or 31%. Table 1 shows the installed capacity of the power plants and the current actual generation in Nigeria; while table 2 shows the generation capacity of new plants under construction.

Table 1: Power Generation capacity of the current Nigeria power grid

S/N	Station	State	Turbine	Installed Capacity (MW)	Available Capacity (MW)
1	Kanji	Niger	Hydro	760	253
2	Jebba	Niger	Hydro	578	351
3	Shiroro	Niger	Hydro	600	402
4	Egbin	Lagos	Steam	1320	900
5	Trans-Amadi	Rivers	Gas	100	57.30
6	A. E. S.	Lagos	Gas	302	211.80
7	Sapele	Delta	Steam	1020	170
8	Ibom	Akwa Ibom	Gas	155	25.30
9	Okpai (Agip)	Delta	Gas	480	221
10	Afam I – V	Rivers	Gas	726	60
11	AfamVI (Shell)	Rivers	Gas	650	510
12	Delta(I-IV)	Delta	Gas	912	281
13	Geregu	Kogi	Gas	414	120
14	Omoku	Rivers	Gas	150	53
15	Omotosho	Ondo	Gas	335	88.30
16	Olorunshogbo Phase I	Ogun	Gas	135	54.30
17	Olorunshogbo Phase II	Ogun	Gas	200	105.50
18	Papalanto		Gas	335	
19	Rain/Ube		Gas	225	
	Total Power (P_1)			**9,397MW**	**3863.5 MW**

Table 2: Generation capacity of new plants under construction.

Station	State	Turbine	Installed capacity, MW
Calabar	Cross River	Gas	561
Egbema	Imo	Gas	338
Ihorbor	Edo	Gas	451
Gbarian	Bayelsa	Gas	225
Alaoji	Abia	Gas	504
Eket	Akwa Ibom	Gas	500
Obite		Gas	450
Total (P_2)			**3,029MW**
Grand Total (P_1+P_2)			**12,426MW**

Omoku generating station and Trans-Amadi generating station are in reality connected to the distribution network through 33KV lines. The actual connection point and parameters of the lines were not available in the data collected.

As shown in table 1, the average availability of the power plant is around 31%. This according to information from PHCN(Power Holding Company of Nigeria) is due to faulty generators, lack of machine maintenance and generally aging generators in the old power plants e.g., Kainji hydro power plant which was commissioned in 1968.

There are a number of governments owned and independent power plant projects under way to expand the generation and consequently the grid as indicated in table 2, and expected to be connected to the grid between 2012 and 2020.

This installed capacity of existing and ongoing Nigerian power plants are estimated at 12,426MW. This means that even with new plants and transmission lines being added, there may still be inefficient generation and transmission capacities due to demand increase.

III. PRESENT LOAD PROJECTION

The word load is used to represent the present power consumption in the system and demand is used to mean the actual power need and future power consumption of the country. At present, only 30%, which is approximately 3,600MW, of the actual electric load of 12,000MW is supplied by the system. The projected demand for the country in 2011 is approximately 12,000MW.

Table 3 shows the load nodal distribution for the demand forecast for years 2012, 2015 and 2020. The forecast was obtained from power presentation on demand forecast done by the Nigerian society of Engineers for PHCN.

In table 3, the column 'current' represents the current load which is been served in the system. The values were obtained from the load allocation of a typical day that was provided by the Transmission System Operator.

Table 3: Load /demand nodal distribution.

Station	Current (MW)	% total load	2012	2015	2020
B.kebbi	124.40	3.45	454.21	631.07	1093.80
Jebba T.S	7.47	0.21	27.27	37.89	65.68
Osogbo	129.77	3.60	473.82	658.31	1141.02
Ayede	190.43	5.28	695.30	966.03	1674.38
Sakete	140.43	3.89	511.17	710.20	1230.97
Ikeja west	230.78	6.40	842.62	1170.72	2029.16
Akangba	247.62	6.87	904.11	1256.15	2177.23
Aja	200.00	5.55	730.24	1014.58	1758.53
Egbin	200.00	5.55	730.24	1014.58	1758.53
Ganmo	42.83	1.19	156.38	217.27	376.59
Kaduna	203.71	5.65	743.79	1033.40	1791.15
Shiroro	73.39	2.04	267.96	372.30	645.29
Katampe	280.00	7.77	1022.34	1420.41	2461.94
Jos	82.59	2.29	301.55	418.97	726.18
Kano	292.66	8.12	1068.56	1484.63	2573.25
Benin	173.08	4.80	631.95	878.02	1521.83
Ajaokuta	68.16	1.89	248.87	345.77	599.31
Gombe	74.81	2.08	273.15	379.50	657.78
New Heaven	113.05	3.14	W	573.49	994.01
Onitsha	130.51	3.62	476.52	662.06	1147.53
Aalaoji	219.79	6.10	802.50	1114.97	1932.53
Eket	50.50	1.40	184.39	256.18	444.03
Yola	26.29	0.73	95.99	481.57	834.68
Maiduguri	14.70	0.41	53.67	133.37	231.16
Port –Harcourt	94.93	2.63	364.61	74.57	129.25
Auxiliary	192.00	5.33	701.03	973.99	1688.19
TOTAL (MW)	**3,603.47**	**100.00**	**13,157.00**	**18,280.00**	**31,684.00**

4. MATERIALS AND METHODS

The MATLAB/SIMULINK Power System Analysis TOOLBOX (PSAT) programme that uses continuation power flow (CPF) methods is deployed to investigate the present voltage stability Nigeria Power System.

4.1 Continuation Power Flow Method Formulation

One important application of power flow studies is to trace and predict the power system's response to load variation in order to avoid system collapse and to ensure the security, economy and control of electrical energy distribution.

The evaluation of the power-voltage or P-V characteristic curve, presented in fig.1, provides crucial information concerning voltage stability and loadability limits at steady-state conditions; while fig.2 shows a typical sequence of calculation using predictor/corrector method. At the tip of the curve, the system reaches its critical point of operation where, normally, it can no longer meet the demand for reactive power. Thus, the upper curve represents the stable operation, while the bottom segment is the unstable region.

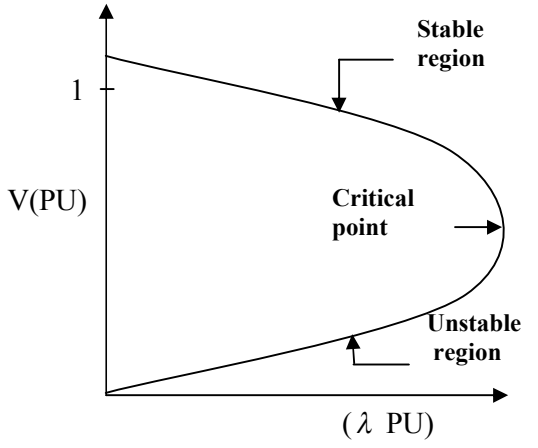

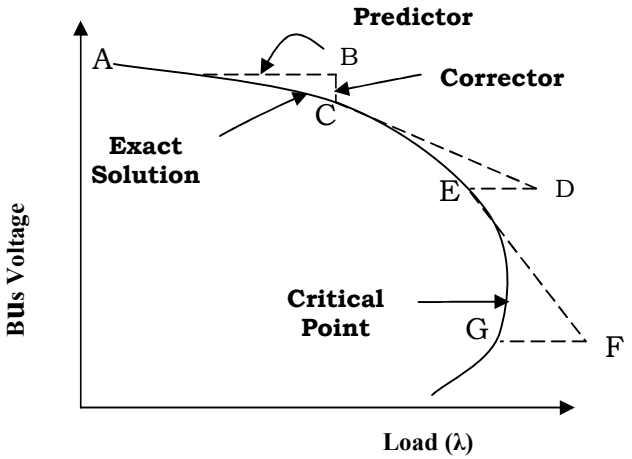

Fig.1: Typical Power-voltage (P-V) curve. Fig. 2: The predictor/corrector steps

The purpose of continuation power flow is to trace the power flow solutions as the loading parameter lambda λ varies. It is numerically difficult to obtain a power flow solution near the voltage collapse point, since the Jacobian matrix becomes singular. Continuation power flow is a technique by which the power flow solution can be obtained near or at the voltage collapse point [6, 11, 12].

There are essentially two phases in the CPF computation: Predictor and Corrector. Basically, the predictor starts from a known solution and forecasts the next equilibrium point. Then, a corrector algorithm based on Newton-Raphson method, makes successively adjustments to state variables until correct continuation power flow solution is reached.

The principles of continuation power flow method are explained as follows:

Locally Parameterized Continuation:

The continuation method uses the conventional Newton Raphson's power flow solution to compute the base parameter. The original system of nonlinear equations is given by:

$$F(x) = 0 \quad (1)$$

The extra variable called a load parameter, λ, is introduced into the original system of nonlinear equation as follows:

$$F(x, \lambda) = 0 \quad (2)$$

Local parameterization allows both the added load parameter, λ and the state variables to be used as continuation parameters.

Mathematical Reformulation of Power Flow Equations:

The continuation method introduces an additional equation and an unknown variable into the basic power flow equation. The reformulation power equation is done by expressing the load and the generation at a bus as a function of the load parameter, λ.

The general forms of the new equations for each bus i are:

$$\Delta P_i = P_{Gi}(\lambda) - P_{Li}(\lambda) - P_{Ti} = 0 \quad (3)$$

$$\Delta Q_i = Q_{Gi}(\lambda) - Q_{Li}(\lambda) - Q_{Ti} = 0 \quad (4)$$

Where:

$$P_s = P_i = P_{Ti} = P_{Gi}(\lambda) - P_{Li}(\lambda) = \sum_{j=1}^{n} V_i V_j Y_{ij} \cos(\theta_i - \theta_j - \theta_{ij})$$

$$Q_s = Q_i = Q_{Ti} = Q_{Gi}(\lambda) - Q_{Li}(\lambda) = \sum_{j=1}^{n} V_i V_j Y_{ij} \sin(\theta_i - \theta_j - \theta_{ij})$$

Where:

λ is the load parameter, which is $0 \leq \lambda \leq \lambda_{max}$ meaning $\lambda = 0$ Corresponding to base case and $\lambda = \lambda_{max}$ corresponding to maximum loading point.

P_i = Injected active power at bus i

Q_i = Injected reactive power at bus i

P_{Gi} = Active power generation at bus i

Q_{Gi} = Reactive power generator at bus i

P_{Li} = Active power load at bus i

Q_{Li} = Reactive power load at bus i.

V_i = Voltage magnitude at bus i

V_j = Voltage magnitude at bus j

θ_i = Voltage angle at bus i

θ_j = Voltage angle at bus j

$Y_{ij} = (i, j)$ Elements of the admittance matrix $[Y_{bux}]$

y_{ij} = Admittance angle

To simulate different load change scenarios, the active power load, P_{Li} and reactive power load, Q_{Li} at bus i are modified as follows:

$$P_{Li} = P_{LiO} + \lambda(K_{Li} S_{\Delta base} \cos\varphi_i) \quad (5)$$

$$Q_{Li} = Q_{LiO} + \lambda(K_{Li} S_{\Delta base} \sin\varphi_i) \quad (6)$$

Where:

$$S_{\Delta base} \cos\varphi_i = P_{LiO}$$

$$S_{\Delta base} \sin\varphi_i = Q_{Lio}$$

Equations (5) and (6) can be rewritten as

$$P_{Li}(\lambda) = P_{Lio}(1 + \lambda K_{Li}) \quad (7)$$

$$Q_{Li}(\lambda) = Q_{Lio}(1 + \lambda K_{Li}) \quad (8)$$

Where:

K_{Li} = Rate of load change at bus i, as λ changed.

P_{Lio}, Q_{Lio} = Original load at bus i active and reactive powers respectively.

$S_{\Delta base}$ = Apparent power at original load.

Q_i = Power factor angle of load at bus i.

Letting $Q_{Lio} = P_{Lio} \tan Q_i$ into equation (8) gives

$$Q_{Li}(\lambda) = P_{Lio} \tan Q_i \ (1 + \lambda K_{Li}) \quad (9)$$

The active power generation, P_{Gi} is modified as follows.

$$P_{Gi}(\lambda) = P_{Gio}(1 + \lambda K_{Gi}) \quad (10)$$

Where:

$P_{Gio}(\lambda)$= Active power generation at base case.

K_{Gi} = Constant specifying rate of change in generation corresponding to λ change.

Power flow equations can be represented as,

$$P_s = P(\theta, V) and\ Q_s = Q(\theta, V) \quad (11)$$

Where P_s, Q_s are specified active and reactive powers of buses, θ and V are bus voltage angles and magnitudes respectively.

Equation (11) can be expressed as,

$$F(\theta, V) = PQ_{spc} = [P_s, Q_s]^T \quad (12)$$

The application of a continuation algorithm:

The power flow equations are reformulated in order to explain the step – by - step algorithm for usage in the continuation power flow. Considering variation of load as one of the parameters of the power flow equations, equation (12) can be rewritten as,

$$F(\theta, V) = \lambda PQ_{spc} = \lambda[P_s, Q_s]^T$$

$$or\ F(\theta, V) - \lambda[P_s, Q_s]^T = 0 \quad (13)$$

$where\ \lambda$ is the loading parameter. For base case loading, λ=1.

Equation (13) can be written as,

$$F(\theta,V,\lambda) = 0,\ 0 \le \lambda \le \lambda_{critical} \quad (14)$$

The whole set of power flow equations represented by F is a set of nonlinear algebraic equations. The base case solution, which is $(\theta_0, V_0, \lambda_0)$, is known from a conventional power flow and the power flow solution path is being sought over a range of loading parameter λ. In general, the dimensions of F will be $2n_1 + n_2$, *where* n_1 *and* n_2 are the number of PQ and PV buses respectively.

C.1. Continuation Power Flow Jacobian Matrix Computation:

The Jacobian matrix $[J]$ of the reformulated power flow equation F(θ, V, λ) = 0 is determined as follows:

$$[J] = \begin{bmatrix} \frac{\partial P_1}{\partial \theta_1} & \cdots & \frac{\partial P_1}{\partial \theta_n} & \frac{\partial P_1}{\partial V_1} & \cdots & \frac{\partial P_1}{\partial V_n} & \\ \vdots & & \vdots & \vdots & & \vdots & \\ \frac{\partial P_n}{\partial \theta_1} & \cdots & \frac{\partial P_n}{\partial \theta_n} & \frac{\partial P_n}{\partial V_1} & \cdots & \frac{\partial P_n}{\partial V_n} & \\ \frac{\partial Q_1}{\partial \theta_1} & \cdots & \frac{\partial Q_1}{\partial \theta_n} & \frac{\partial Q_1}{\partial V_1} & \cdots & \frac{\partial Q_1}{\partial V_n} & \frac{\partial \theta_1}{\partial \lambda} \\ \vdots & & \vdots & \vdots & & \vdots & \\ \frac{\partial Q_n}{\partial \theta_1} & \cdots & \frac{\partial Q_n}{\partial \theta_n} & \frac{\partial Q_n}{\partial V_1} & \cdots & \frac{\partial Q_n}{\partial V_n} & \\ & & & \vdots & & & \end{bmatrix} \quad (15)$$

The Jacobian matrix of the reformulated power flow equations (3) and (4) for each PV and PQ buses is computed based on base case parameter value λ.

The minimum singular value σ_{min} is computed as follows:

$$\sigma_{min} = \|[J]^{-1}\|^{-1} \quad (16)$$

The tangent vector computation, predictor, and corrector continuation techniques are deployed to find subsequent solutions at different load levels.

C.2. Tangent Vector Computation:

The predictor process is deployed to calculate the tangent vector. This tangent vector calculation is derived by first taking the partial derivation of both sides of F, which is the power flow equation (14) with respect to θ, V and λ.

Hence, $\Delta F = \frac{\partial F}{\partial \theta}\Delta\theta + \frac{\partial F}{\partial V}\Delta V + \frac{\partial F}{\partial \lambda}\Delta\lambda$ (17a)

$$or, dF = \frac{\partial F}{\partial \theta}d\theta + \frac{\partial F}{\partial V}dV + \frac{\partial F}{\partial \lambda}d\lambda = 0 \quad (17b)$$

$$or, d[F(\theta,V,\lambda)] = F_\theta d\theta + F_V dV + F_\lambda d\lambda = 0 \quad (17c)$$

Now,

$$\Delta F = F(\theta_0,V_0,\lambda_0) - F(\theta,V,\lambda) = -F(\theta,V,\lambda) \quad (18)$$

where $(\theta_0, V_0, \lambda_0)$ is the solution of equation (14).

Using the above in equation (17) and writing in matrix form, gives

$$\begin{bmatrix} \frac{\partial F}{\partial \theta} & \frac{\partial F}{\partial V} & \frac{\partial F}{\partial \lambda} \end{bmatrix} \begin{bmatrix} \Delta\theta \\ \Delta V \\ \Delta\lambda \end{bmatrix} = [-F(\theta,V,\lambda)] \quad (19a)$$

$$or, \begin{bmatrix} \frac{\partial F}{\partial \theta} & \frac{\partial F}{\partial V} & \frac{\partial F}{\partial \lambda} \end{bmatrix} \begin{bmatrix} d\theta \\ dV \\ d\lambda \end{bmatrix} = [-F(\theta,V,\lambda)] \quad (19b)$$

$$or, [F_\theta F_V F_\lambda] \begin{bmatrix} d\theta \\ dV \\ d\lambda \end{bmatrix} = [-F(\theta,V,\lambda)] \quad (19c)$$

This can be written as,

$$J.[\Delta\theta\ \Delta V\ \Delta\lambda]^T - [-F(\theta,V,\lambda)]$$
$$or,\ [\Delta\theta\ \Delta V\ \Delta\lambda]^T = J^{-1}.[-F(\theta,V,\lambda)] \quad (20a)$$
$$or,\ J.[d\theta\ dV\ d\lambda]^T = [-F(\theta,V,\lambda)]$$
$$or,\ [d\theta\ dV\ d\lambda]^T = J^{-1}.[-F(\theta,V,\lambda)] \quad (20b)$$

Where, J is the Jacobian matrix.

$[\Delta\theta\ \Delta V\ \Delta\lambda]^T or [d\theta\ dV\ d\lambda]^T$ is the tangent vector being sought.

$[F_\theta F_V F_\lambda]$ is the partial derivative of F with respect to θ, V, λ.

Near the point of voltage collapse, the Jacobian matrix, J approaches singularity; hence it is difficult to calculate J^{-1} near the collapse point. This problem is solved by setting one of the components of tangent vector, say dλ as ±1, depending on where the solutions curve changes. When the tangent vector, dλ is equal to +1, the solution curve increases and when dλ is equal to -1, the solution curve decreases. This fixed variable is called the continuation variable. Assuming that the i^{th} variable is the continuation variable, one can write,

$$[e_i][\Delta\theta\ \Delta V\ \Delta\lambda]^T = 0 \quad (21a)$$
$$or, [e_i][d\theta\ dV\ d\lambda]^T = 0 \quad (21b)$$

where $[e_i]$ is the vector having i^{th} element as one and all other elements as zero.

Rewriting equation (21), gives

$$\begin{bmatrix} J \\ e_i \end{bmatrix}[\Delta\theta\ \Delta V\ \Delta\lambda]^T = \begin{bmatrix} -F(\theta,V,\lambda) \\ 0 \end{bmatrix} \quad (22a)$$

$$or, \begin{bmatrix} J \\ e_i \end{bmatrix}[d\theta\ dV\ d\lambda]^T = \begin{bmatrix} -F(\theta,V,\lambda) \\ 0 \end{bmatrix} \quad (22b)$$

C.3. Predictor Step:

The difference vector $[\Delta\theta\ \Delta V\ \Delta\lambda]^T or\ [d\theta\ dV\ d\lambda]^T$ is found from equation (22) and added with the initial assumption of vector $(\theta_0\ V_0\ \lambda_0)$ to get the predictor. That is, the predicted value is calculated by:

$$\begin{bmatrix} \theta \\ V \\ \lambda \end{bmatrix}^{predicted} = \begin{bmatrix} \theta_0 \\ V_0 \\ \lambda_0 \end{bmatrix} + h \begin{bmatrix} \Delta\theta \\ \Delta V \\ \Delta\lambda \end{bmatrix}^T \quad (23a)$$

$$or, \begin{bmatrix} \theta \\ V \\ \lambda \end{bmatrix}^{predicted} = \begin{bmatrix} \theta_0 \\ V_0 \\ \lambda_0 \end{bmatrix} + h \begin{bmatrix} d\theta \\ dV \\ d\lambda \end{bmatrix}^T \quad (23b)$$

Where, h is a scalar quantity representing the step size. In this study, the step size, h is assigned a constant value of 0.001. Hence, the procedures involved in predictor step are

summarized as follows: specifying the step size h; finding the partial derivatives of F(θ, V, λ) with respect to θ, V and λ respectively; using the step size h and partial derivatives to find the next point or predicted value (θ, V, λ).

C.4. Corrector step:

The predictor may not be exactly on the desired power flow solution curve. To get the exact power flow solution curve, the following corrector equations are added with the set of equations of F(θ, V, λ) = 0, $0 \leq \lambda \leq \lambda_{critical}$.

$$X_i = \mu^{predicted} \; or \; X_i - \mu^{predicted} = 0 \quad (24)$$

$where\ \mu$ is the assumed fixed/predicted value of the continuation variable, and X_i is the state variable chosen as continuation parameter.

Thus, the system equations become,

F(θ, V, λ) = 0 and, $X_i - \mu^{predicted} = 0$ (25a)

$$or, F(X, \lambda) = 0 \; and, X_i - \mu^{predicted} = 0 \quad (25b)$$

$$or, \begin{bmatrix} F(X, \lambda) \\ X_i - \mu \end{bmatrix} = 0 \quad (25c)$$

(D) Selecting the continuation parameter:

The best method of selecting the correct continuation parameter at each step is to select the state variable with the largest tangent vector component. To begin with the load parameter λ is a good choice, and subsequent continuation parameters can be evaluated as:

$$x_K : |t_K| = \max \{|t_1|, |t_2|, \ldots, |t_m|\} \quad (26)$$

Here, t is the tangent vector. After the continuation parameter is selected, the proper value of either $+1$ or -1 should be assigned to t_K in the tangent vector calculation.

(E) Identifying the Critical Point:

The critical point is the point where the loading has maximum value. After this point, it starts to decrease. The tangent component of λ is zero at the critical point and negative beyond this point. Therefore, the sign of $d\lambda$ shows whether the critical point is reached or not.

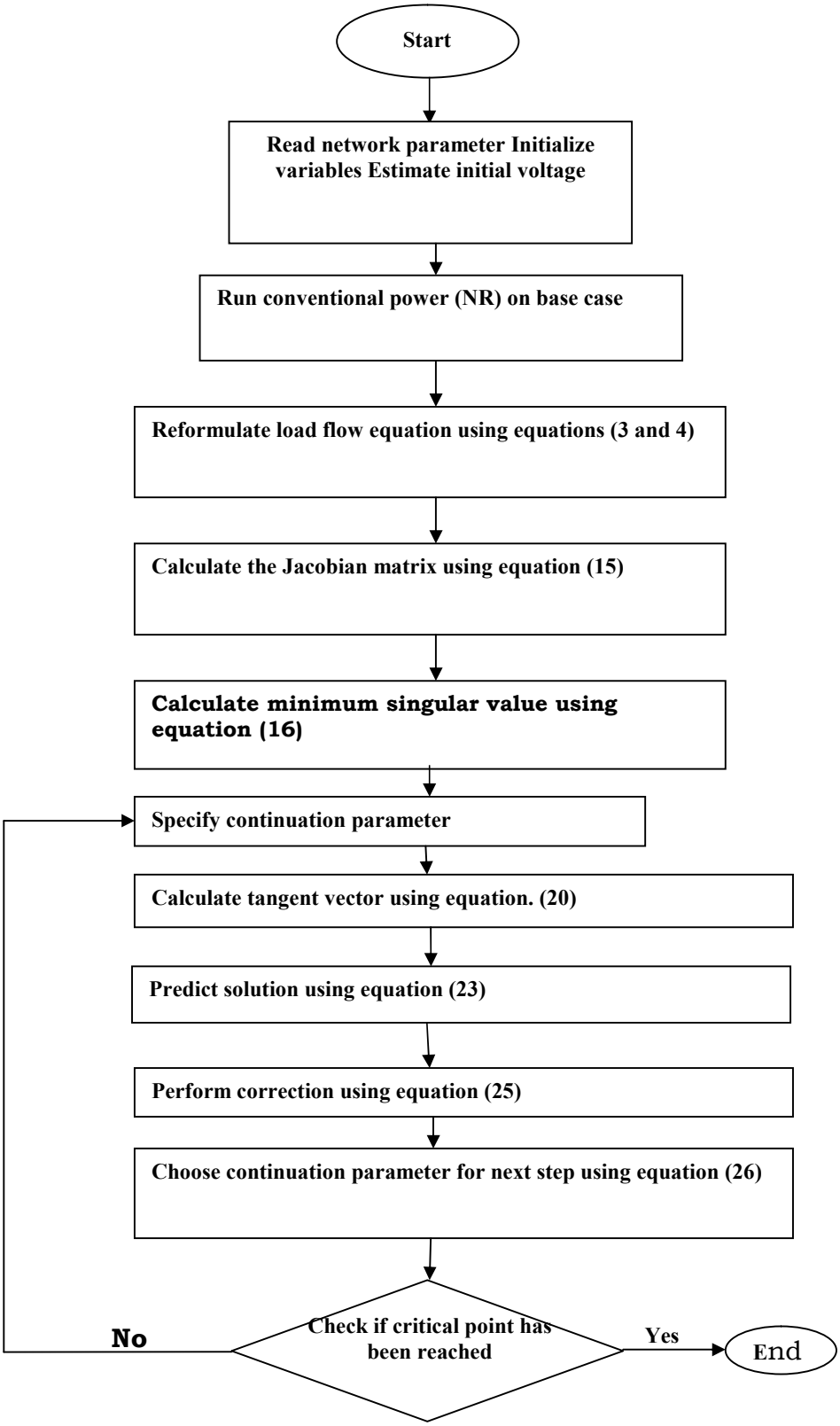

Fig. 3 shows a flow chart for a continuation power flow.

4.2 Application of Power Flow and Continuation Power Flow Methods to Investigate Voltage Stability of 28-bus, 330KV Nigeria Power System

Fig. 4 shows 330KV, 28-bus, Nigeria Power Network consisting of 28 nodes, 10 generators, 18 load (PQ) buses, 16 transformers, 12,426MW grid capacity and 5,988km grid transmission lines. The network has a total load of 2,468.06MW and 1,851.05Mvar. The system bus no.1 is chosen as slack bus, buses no.2 to bus.10 are PV buses, while buses 11 to 28 are PQ (load) buses. The continuation power flow method uses the conventional Newton-Raphson method at the base case where $\lambda = \lambda_0 = 0$ to compute the power load data. Then, the state variable related to the load is increased. Before reaching the critical (knee) point, the system is affected more by other state variables like voltage or delta. This is because at the critical (knee) point, the voltage changes rapidly for very small change in power.

MATLAB/SIMULINK model/diagram of voltage stability investigation of 28- bus grid network using continuation power flow method is presented in fig.5. The input data for the power flow analysis and CPF method includes: bus data and line data consisting of generator's output power, maximum and minimum reactive power limit of the generator, MW and Mvar peak loads, impedance of the lines, transmission line sizes, voltage and power ratings of the line and transformer data, and the nominal and critical voltages of each of the buses, which is presented in tables 4 to 6 respectively.

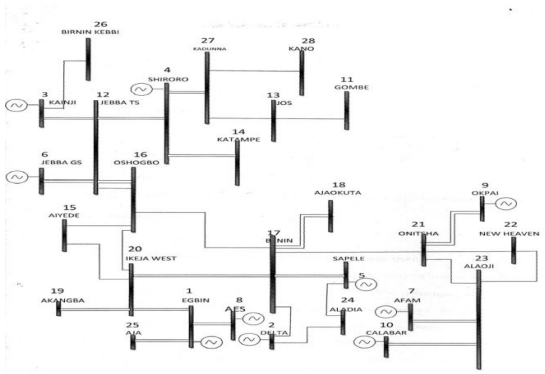

Fig. 4:The existing 28 bus 330KV Nigeria Power Network

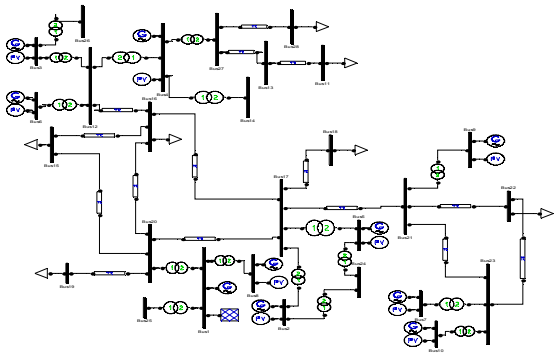

Fig. 5: SIMULINK model of the 330KV Nigeria Power Network.

Table 4: Generator Data

BUS NUMBER	BUS NAME	P_G (MW)	VOLTAGE (PU)
1	Egbin	1320	1
2	Delta PS	900	1
3	Kaniji	760	1
4	Shiroro	600	1
5	Sapele	1020	1
6	Jebba GS	578	1
7	Afam GS	726	1
8	AES	302	1
9	Okpai	480	1
10	Calabar	563	1

Table 5: Load data

BUS NO	BUS NAME	ACTIVE POWER (MW)	REACTIVE POWER (MVAR)	BUS NO	BUS NAME	ACTIVE POWER (MW)	REACTIVE POWER (MVAR)
11	Gombe	130	80	20	Ikeja west	484	300
12	Jebba TS	7.44	3.79	21	Onitsha	146	77
13	Jos	114	90	22	New Haven	182	112
14	Katampe	236	146	23	Alaoji	248	153
15	Aiyede	210	130	24	Aladja	47.997	24.589
16	Oshogbo	194	120	25	Aja	200	124
17	Benin	136	84	26	Brini-Kebbi	89	55
18	Ajaokuta	72	45	27	Kaduna	260	161
19	Akanagba	389	241	28	Kano	226	140

Table 6: Lines and transformer data

FROM BUS	TO BUS	r(PU)	X(PU)	Y/2 (PU)	FROM BUS	TO BUS	r(PU)	X(PU)	Y/2 (PU)
1	8	0.0001	0.0004	0.0996	10	23	0.0163	0.014	0.786
1	20	0.0004	0.0029	0.771	11	13	0.0032	0.0027	1.515
1	25	0.0007	0.0057	0.3855	12	16	0.0019	0.0159	0.8955
2	17	0.0008	0.0063	0.3585	13	27	0.0027	0.0202	1.2114
2	24	0.0008	0.0063	0.3585	15	16	0.0013	0.010	0.5999
3	26	0.0041	0.0304	1.8135	15	20	0.0016	0.0134	0.0857
3	12	0.001	0.0082	0.924	16	17	0.003	0.0254	1.431
4	27	0.0011	0.0097	0.546	16	20	0.0033	0.0227	1.4819
4	12	0.0022	0.0234	1.3905	17	18	0.0023	0.0198	1.11117
4	14	0.0009	0.0067	1.7933	17	20	0.0034	0.0016	1.7015
5	17	0.0002	0.0015	0.936	17	21	0.0016	0.0139	0.781
5	24	0.0008	0.0063	0.3585	19	20	0.0007	0.0057	0.3855
6	12	0.0001	0.0004	0.0996	21	22	0.0011	0.0097	0.5475
7	23	0.0015	0.0012	0.312	21	23	0.0163	0.014	0.786
9	21	0.0008	0.0063	0.3585	22	23	0.0023	0.0171	1.3905
					27	28	0.0027	0.0202	1.2114

5. RESULTS AND DISCUSION

5.1 CONTINUATION POWER FLOW RESULTS OF 28 – BUS TEST SYSTEM

The results of the continuation power flow of the 28 bus system performed under base case/normal operating conditions, loss of a generator and loss of a transmission line are indicated by the power-voltage (P-V) curves and voltage profiles of the system as shown in figs. 4 to 11 respectively.

Fig. 4 shows the power-voltage (P-V) curve of 28 - bus system performed using continuation power flow method under base case/normal operating conditions. Fig. 5 shows variation of bus voltage with increasing load factor, λ on the 28-bus system under base case/normal operating conditions.

From figs. 4 and 5 respectively, it can be seen that the weakest bus is bus 3 (Kainji GS) with voltage profiles of 0.5845 PU (193KV), while other weak buses include bus 5 (Sapele PS) and bus 21 (Onitsha TS) with voltage profiles of 0.61669PU (203.51KV) and 0.68731PU (226.81KV) respectively.

However, the maximum and minimum values for the steady state voltage stability limits are 0.90364PU (298.20KV) and 0.5845PU (193KV) on bus 2 (Delta PS) and bus 3 (Kainji GS) respectively. These voltage stability limits/indices results suggest that voltages at all the 28 buses of the present Nigeria power system are less than the minimum specified value of 0.95PU (313.5KV). It means that voltage profiles at all the 28 buses of the present Nigeria power system are not within the acceptable/permissible range of ±5% tolerance of rated values, that is 0.95PU (313.5KV) to 1.05PU (346.5KV).

After the continuation power flow simulation for the present Nigeria Power Network voltage stability under normal operating conditions, it was observed that all the 28 buses experienced low voltage violations problems, while all the transmission lines were overloaded.

From the P-V curve of fig. 5, the maximum loading/loadability point (MLP), Lamda (λ) of the 28 bus system is 4.7014PU (470.14MW). It means that the maximum power expected for the 28 bus system to be loaded under base case/normal operating conditions is 4.7014PU (470.14MW), beyond which the network might collapse at any time. At the collapse point or maximum loading point only the slack generator supplies the reactive power. Taking a base point of 1PU = 100MW = 100MVar under base case/normal operating conditions, the total maximum active power load, Ptotal is estimated as 25.8818PU (2588.18MW) from the CPF result.

Figs. 6 and 7 show the P-V curves and voltage profiles of 28-bus Nigeria power system operating under base condition.

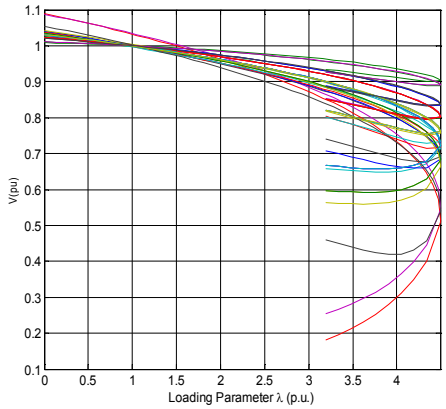

Fig6: Base case P-V curve of 28 bus system

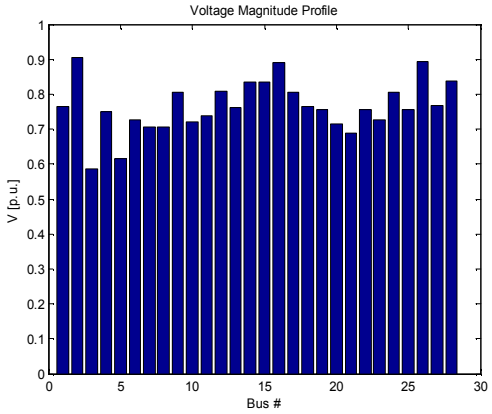

Fig7: Base case Voltage profiles of 28 bus system

Figs. 8 and 9 show the P-V curves and voltage profiles after the loss of generator at bus 2.

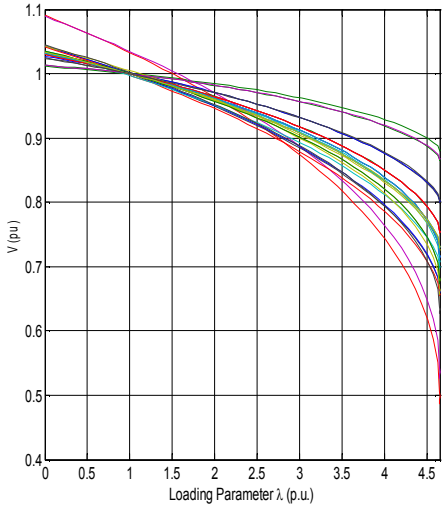

Fig. 8: P – V curve of 28 bus system after loss of generator at bus2.

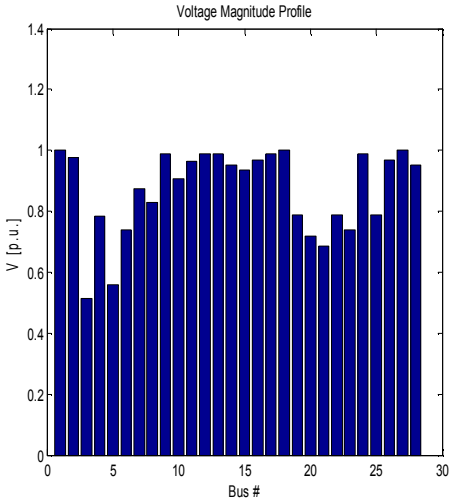

Fig. 9: Voltage profiles of 28 bus system after loss of generator at bus 2.

The weakest bus is bus3 (Kainji GS bus) with voltage profiles of 0.4988pu (164.62KV). Other weak buses include bus5 (Sapele PS bus) and bus21 (Onitsha TS bus) with voltage profiles of 0.53679pu (177.14KV) and 0.63343pu (209.03KV) as shown in figs. 8 and 9 respectively. Figs 10 and 11 show the P-V curves and voltage profiles of the network after the loss of line (1-25).

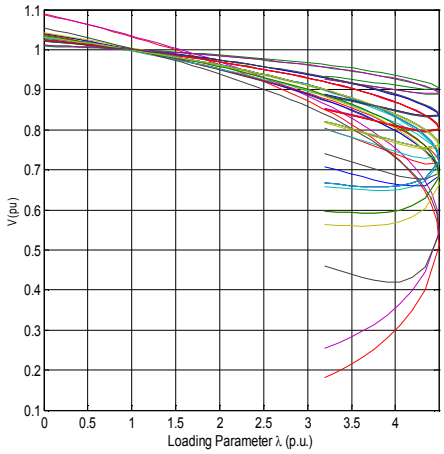

Fig. 10: P-V curve of 28 bus system after loss of line (1-25)

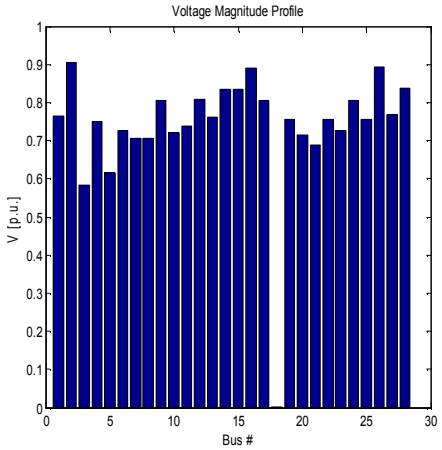

F ig. 11: Voltage profiles of 28 bus system after loss of line (1-25)

The weakest bus is bus3 (Kainji GS bus) with voltage profiles of 0.58475pu (192.97KV). Other weak buses include bus5 (Sapele PS bus) and bus21 (Onitsha TS bus) with voltage profiles of 0.6166pu (203.48KV) and 0.68724pu (226.79KV) as shown in figs. 10 and 11 respectively.

CONCLUSION

The voltage stability investigation results of 28-bus grid network obtained under normal operating conditions revealed that this network is unstable and associated with persistent and frequent occurrences of high power losses and voltage profiles of all buses exceeding ±5% tolerance of the rated value due to inadequate power generation capacity as shown in figs. 4 and 5 respectively. As clearly seen in the voltage stability investigation of 28-bus grid network, this network cannot provide the sufficient power needed to illuminate the entire Nation with increasing system load. Even before the collapse/critical point, 28-bus grid network has many voltage instability problems as the system load increases.

REFERENCES

1. Sambo, A.S., Garba, B., Zarma, I. H. And Gaji, M. M., Electricity Generation and Present Challenges in the Nigeria Power Sector, Energy Commission of Nigeria, Abuja, Nigeria, 2011.
2. Obadote, D. J., Energy Crisis in Nigeria: Technical Issues and Solutions, Power Sector Prayer Conference, June 25-27, 2009.
3. Sambo, A.S., Paper Presented at the National Workshop on the Participation of State Government in the Power Sector: Matching Supply with Demand, Ladi Kwali Hall, Sheraton Hotel and Tower, Abuja, 29 July, 2008.
4. Omorogiuwa,E. And Emmanuel, A. O, Determination of Bus Voltages, Power Loses and Flows in the Nigeria 330KV Integrated Power System, International Journal of Advances in Engineering and Technology, Vol. 4, PP 94-106, June 2012.
5. IEEE/ PES Power System Stability Subcommittee, Voltage Stability Assessment: Concepts Practices and Tools, Special Publication, Final Draft, 2013.
6. Kunder, P., Power System Stability and Control, Mc Graw Hill, 1993.

7. Wener, C. R. And John, V. B, A locally Parameterized Continuation Process, ACM Trans. On Mathematical Software, Vol 9, no 2, PP. 215-235, 1983.
8. Laton, M. Z., Musirin, I. And Abdul Rahman, T. K., Voltage Stability Assessment Via Continuation Power Flow Method, International Journal of Electrical and Electronic Systems Research, Vol. 1, PP 71-78, June 2008.
9. Al-Awami, H. A., Power Flow Control to Determine Voltage Stability Limit by using the Continuation Method, EE 550, 062 Term Paper, Dept. Of Electrical Engineering, KFUPM, 2012.
10. Sode – Yome, A. And Mitulananthan, N., Static Voltage Stability Margin Enhancement Using STATCOM, TCSC and SSSC, IEEE/ PES Conference, Dalian, China, 2005.
11. Cutsem, T. V. And Vournas, C., Voltage Stability of Electric Power Systems, Kluwer Academic Publishers, 1998.
12. Seydel, R., From Equilibrium to Chaos, Elsevier, New York, 1988.